Immunity, Volume *52*

Supplemental Information

Developmental Relationships of Four Exhausted CD8$^+$ T Cell Subsets Reveals Underlying Transcriptional and Epigenetic Landscape Control Mechanisms

Jean-Christophe Beltra, Sasikanth Manne, Mohamed S. Abdel-Hakeem, Makoto Kurachi, Josephine R. Giles, Zeyu Chen, Valentina Casella, Shin Foong Ngiow, Omar Khan, Yinghui Jane Huang, Patrick Yan, Kito Nzingha, Wei Xu, Ravi K. Amaravadi, Xiaowei Xu, Giorgos C. Karakousis, Tara C. Mitchell, Lynn M. Schuchter, Alexander C. Huang, and E. John Wherry

Figure S1, related to main Figure 1.

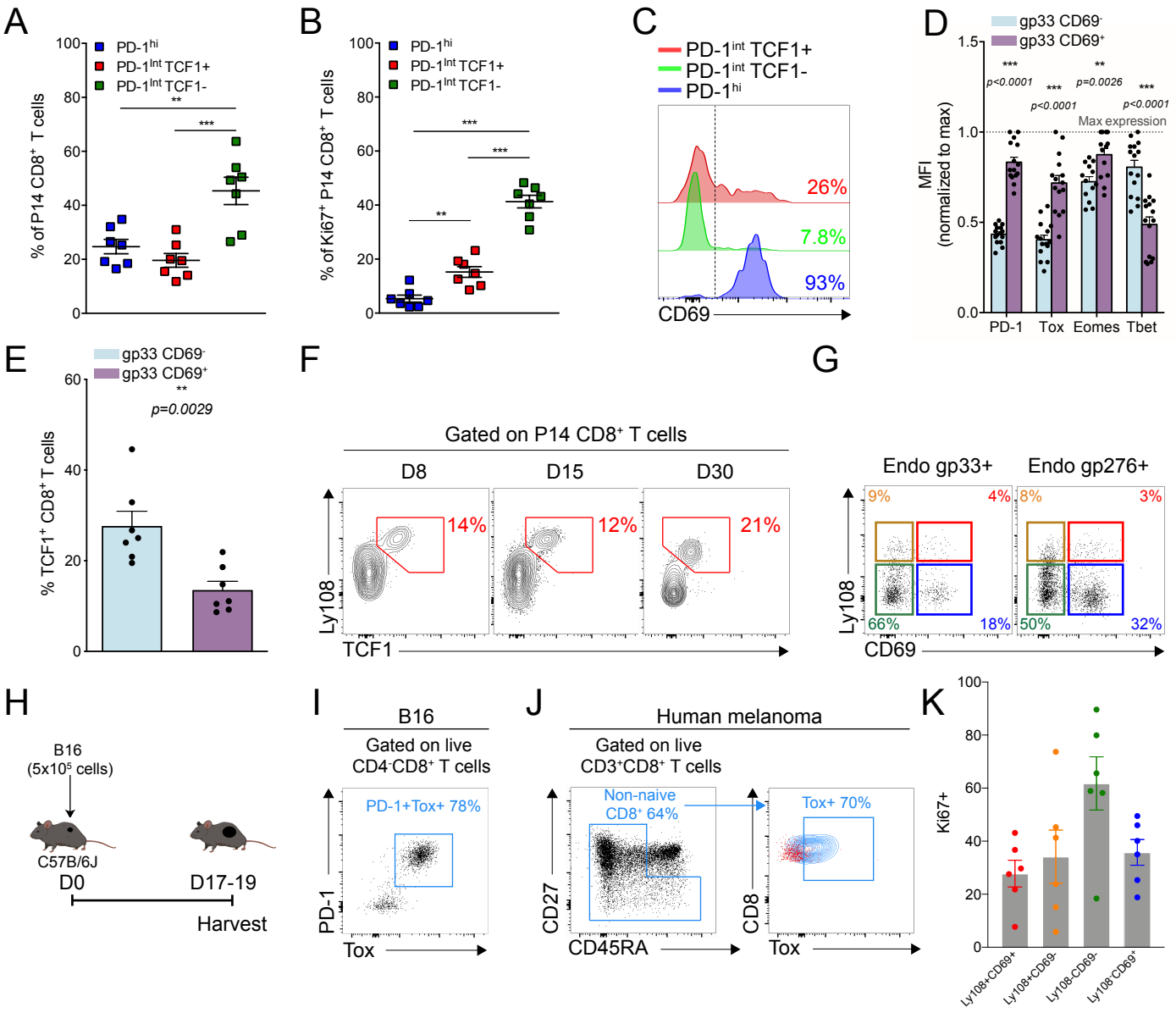

Figure. S1, related to main Figure 1: Ly108 (Slamf6) and CD69 expression delineate Tex subset heterogeneity
(A) Frequencies of indicated populations of P14 CD8⁺ T cells at d30p.i. (B) Frequencies of indicated populations of P14 CD8⁺ T cells expressing Ki67 at d30p.i. (C) Representative CD69 expression by indicated P14 CD8⁺ T cell populations at d30p.i. Numbers indicate frequencies of positive cells. (D) Cumulative MFIs (normalized to max expression/experiment) for indicated markers in indicated populations among endogenous Dbgp33 tetramer⁺ CD8⁺ T cells at d30p.i. (E) Frequencies of TCF1-positive cells among endogenous Dbgp33 tetramer⁺ CD8⁺ T cells that were either CD69- or CD69+ at d30p.i. (F) Representative Ly108 and TCF1 co-expression in P14 CD8⁺ T cells at the indicated time points of LCMV clone 13 infection. Numbers indicate frequencies of double positive cells. (G) Representative Ly108 and CD69 co-expression on indicated tetramer⁺ populations at d30p.i. Numbers indicate frequencies. (H) Experimental design, (I) Gating strategy for CD8⁺ T cells in B16 tumors. (J) Gating strategy for CD8⁺ T cells in human melanoma tumors. Naïve CD8⁺ T cells (red dots) were used to set up the Tox⁺ gate. (K) Frequencies of Ki67⁺ cells among indicated populations of non-naïve (Tox⁺) CD8⁺ T cells isolated from Human melanoma tumors (n=6 patients)
A-G (Representative of n=5 experiments with 16 mice/group)

Figure S2, related to main Figure 2.

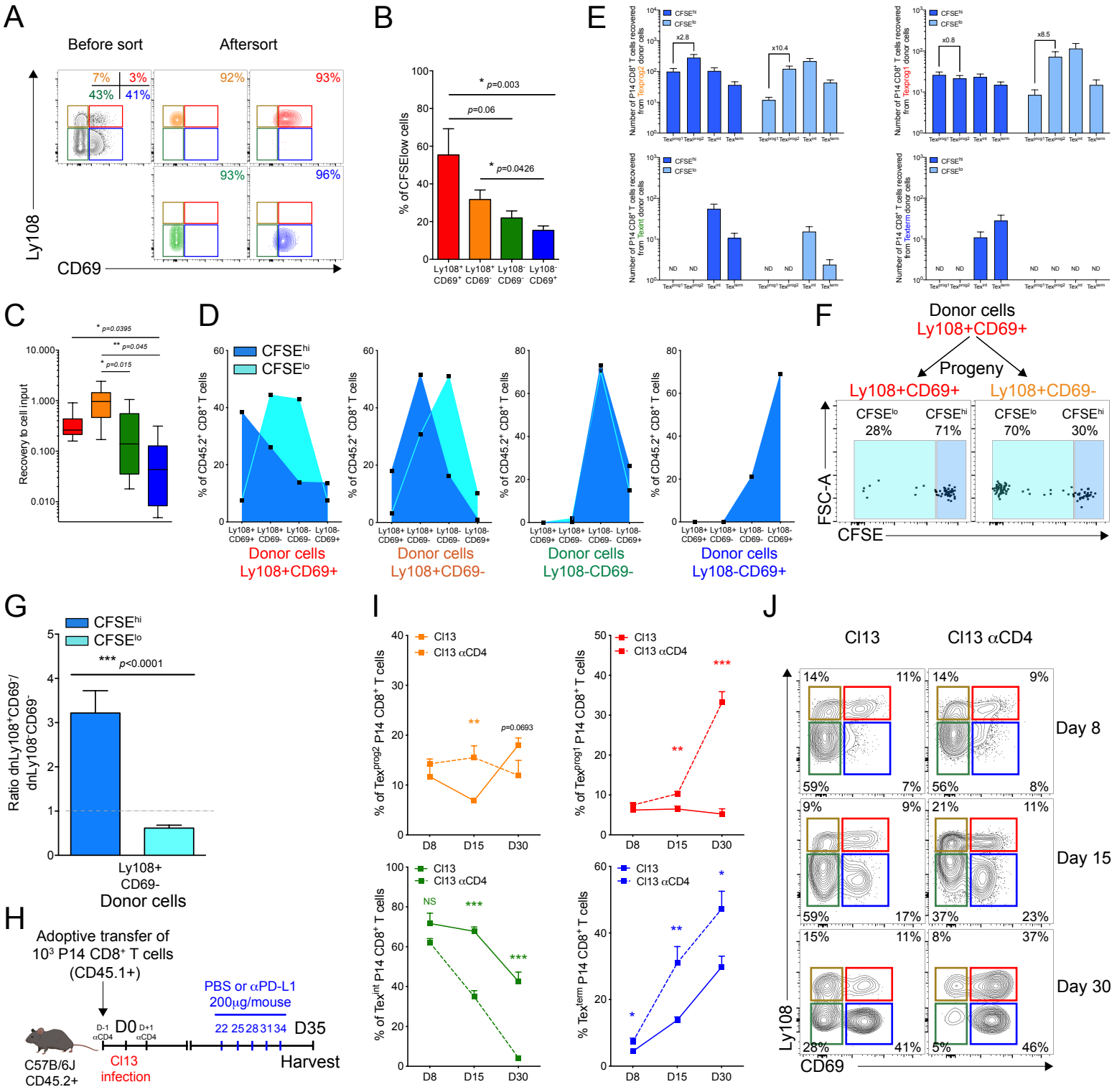

Figure. S2, related to main Figure 2: Tex subset dynamics is altered by the absence of CD4 T cells or PD-L1 blockade
(A) Sort purity (d21p.i.). (B) Frequencies of CFSE^{lo} cells among indicated P14 populations at d28p.i. (d21+7). (C) Percentages of cell-recovery compared to initial cell input. (D) Frequencies of CFSE^{hi} (dark blue) and CFSE^{lo} (light blue) cells within indicated recovered populations from each donor cell-type. (E) Absolute numbers of Tex subsets recovered from the non-dividing (CFSE^{hi}; dark blue) and dividing (CFSE^{lo}; light blue) fraction of indicated donor cell-type. (F) CFSE profile of Ly108^{+}CD69^{+} and Ly108^{+}CD69^{-} cells derived from Ly108^{+}CD69^{+} donor cells at d28p.i. (d21+7). Numbers indicate frequencies. (G) Ratios of de novo Ly108^{+}CD69^{-}/Ly108^{-}CD69^{-} within divided (CFSE^{lo}; light blue) and undivided (CFSE^{hi}; dark blue) Ly108^{+}CD69^{-} donor cells. (H) Experimental design. (I) Frequencies of indicated P14 CD8^{+} T cell populations at indicated time points post infection with LCMV clone 13 (plain line) or clone 13 treated with αCD4 (dotted line). (J) Representative Ly108 and CD69 co-expression on P14 CD8^{+} T cells at indicated time points post infection with LCMV clone 13 (left dots) or clone 13 treated with αCD4 (right dots). Numbers indicate frequencies.
Panels A-G (n=2 with 6-8 mice/group); I-J (n=2 with 7-11 mice/group)

Figure S3, related to main Figure 2.

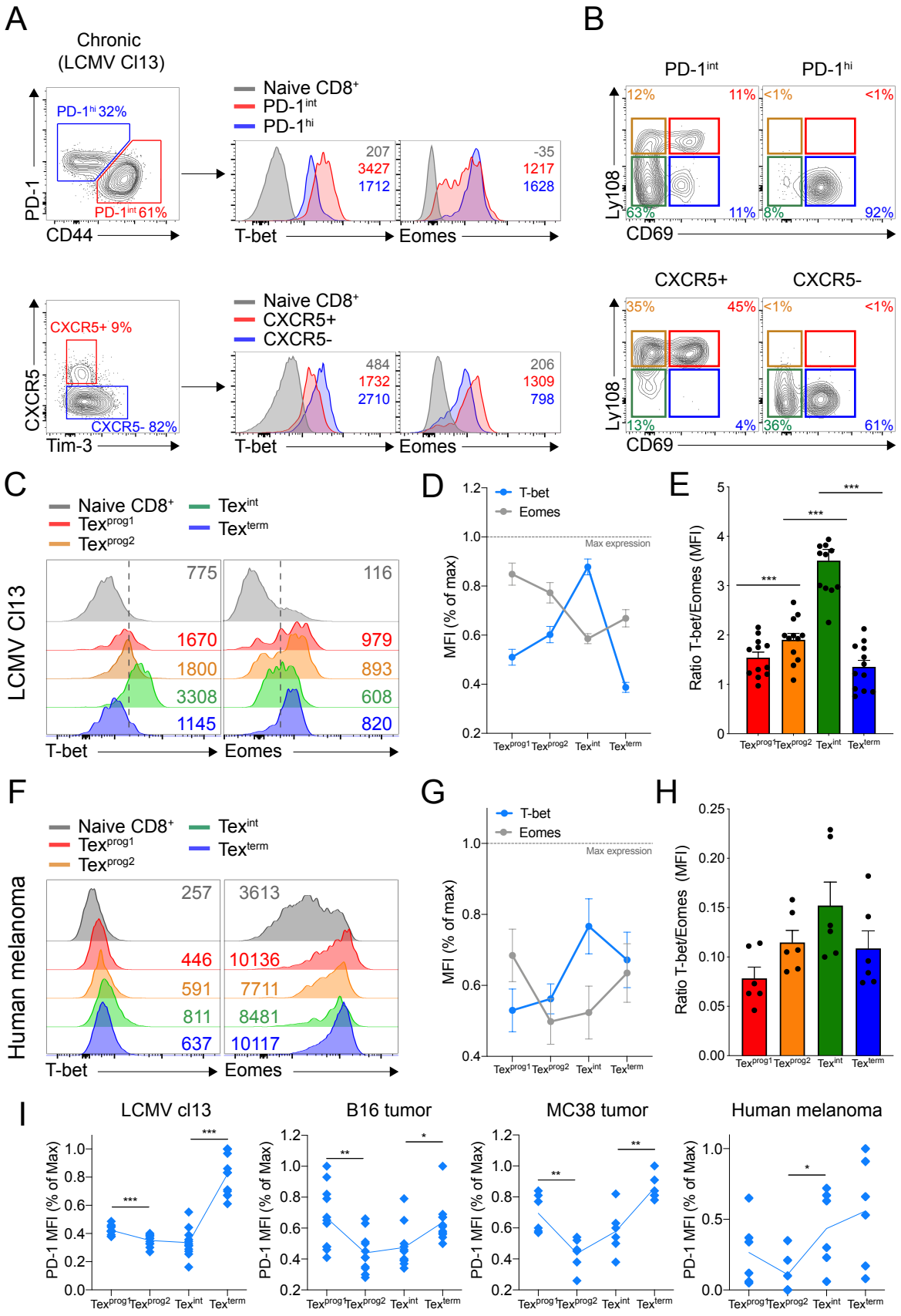

(Legend next page)

Figure. S3, related to main Figure 2: Dynamic T-bet and Eomes expression patterns in Tex subsets

(A) Representative T-bet and Eomes expression in PD-1^{int}/PD-1^{hi} and Cxcr5^{+}/Cxcr5^{-} cells. Numbers indicate frequencies (left dots) or MFI (right histograms). (B) Representative Ly108 and CD69 co-expression by indicated P14 CD8^{+} T cell populations at d30p.i. Numbers indicate frequencies. (C) Representative T-bet and Eomes expression by indicated P14 populations at d30p.i. Numbers indicate MFI. (D) Protein expression dynamics of T-bet and Eomes in indicated P14 populations at d30p.i. (E) Ratios of T-bet/Eomes (MFI) in indicated P14 populations at d30p.i. (F) Representative T-bet and Eomes expression by indicated populations among non-naïve CD8^{+} T cells (Tox^{+}) isolated from Human melanoma tumors. Numbers indicate MFI. (G) Protein expression dynamics of T-bet and Eomes by indicated populations among non-naïve CD8^{+} T cells (Tox^{+}) isolated from Human melanoma tumors. (H) Ratios of T-bet/Eomes (MFI) in indicated populations among non-naïve CD8^{+} T cells (Tox^{+}) isolated from Human melanoma tumors. (I) PD-1 expression dynamic by indicated populations among P14 CD8^{+} T cells (LCMV; d30p.i.) or non-naïve CD8^{+} T cells (Tox^{+}) isolated from indicated tumor type.

Panels A-E (n=3 with 11-12 mice/group)

Panels F-H (n=6 patients)

Panel I (n=2-3 with 6-10 mice/group)

Figure S4, related to main Figure 3.

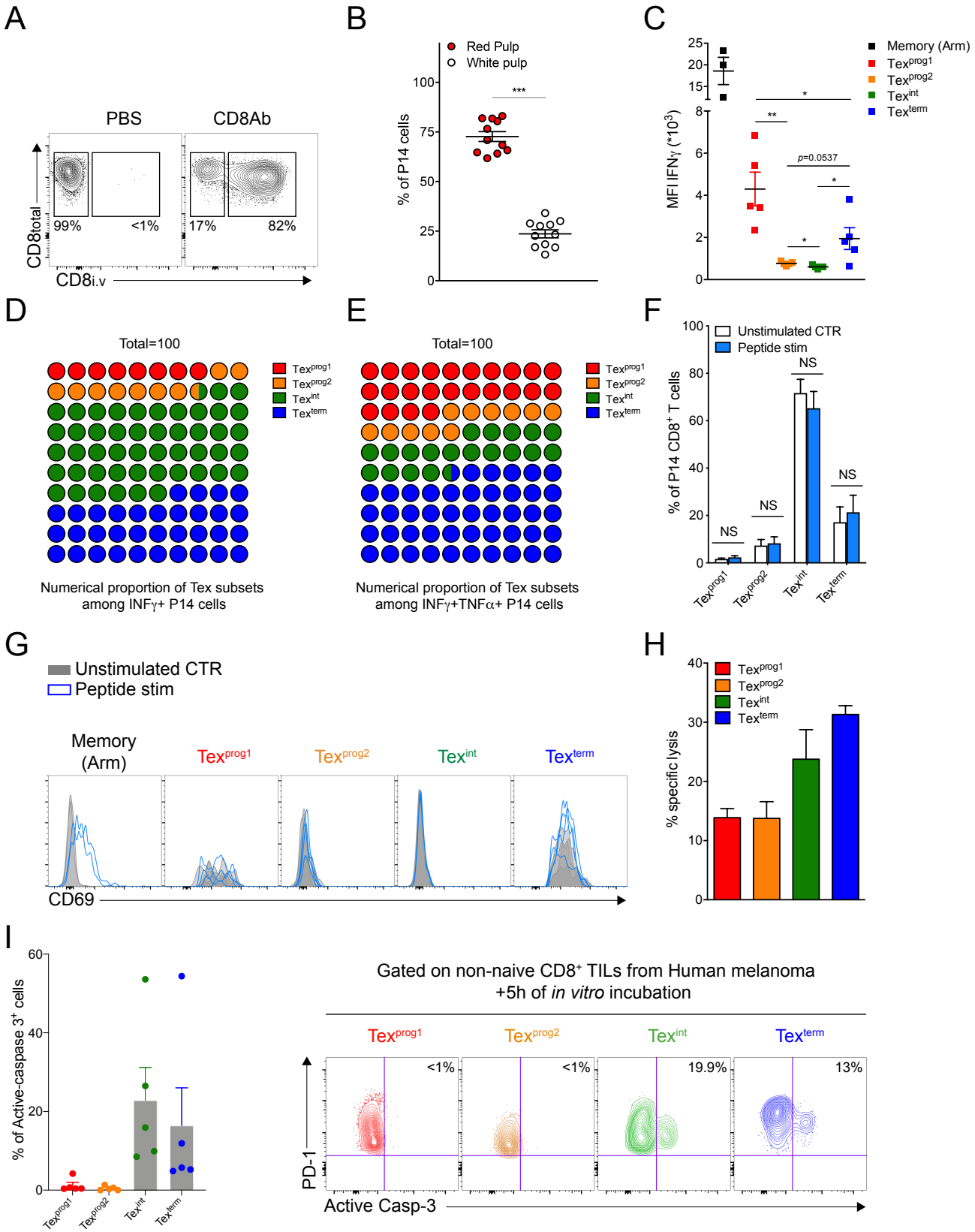

Figure. S4, related to main Figure 3: Tex subsets differ in anatomical localization and effector function.
(A-B) Clone 13 infected mice containing P14 cells were injected i.v. with 3μg/mice of anti-CD8 antibody at d30p.i. and sacrificed three minutes after injection. Representative flow cytometry plots (A) and cumulative frequencies (B) of splenic P14 cells stained (CD8 i.v+, red) or not (CD8 i.v-, open circles) with the in vivo labelling. Numbers indicate frequencies. (C) MFI for IFNγ in indicated P14 populations after 5h of re-stimulation. (D-E) Numerical proportion of IFNγ⁺ Tex cells contributed by each Tex subset (D) or similar analysis for IFNγ⁺TNF⁺ (E) P14 CD8⁺ T cells at d30p.i. (F) Frequency of indicated P14 populations after 5h of culture in re-stimulation medium with (blue bars) or without (open bars) gp33 peptide. (G) Representative CD69 expression in indicated populations after 5h of re-stimulation in media containing (peptide stim; blue) or not (unstimulated CTR; grey) gp33 peptide. (H) Lysis of gp33 loaded target cells by indicated P14 cell populations after 16hours (ratio E/T 3:1). (I) Representative dot plots and frequencies of active caspase-3-positive cells within non-naïve CD8⁺ T cells (Tox⁺) isolated from Human melanoma tumors. Numbers indicate frequencies. (n= 5 patients)
Panels A-B (n=3 with 11-12 mice/group); C-E (n=2 with 7 mice/group); F-G (n=1 with 4 mice/group); H (n=1 with 4 technical replicates)

Figure S5, related to main Figure 4.

(Legend next page)

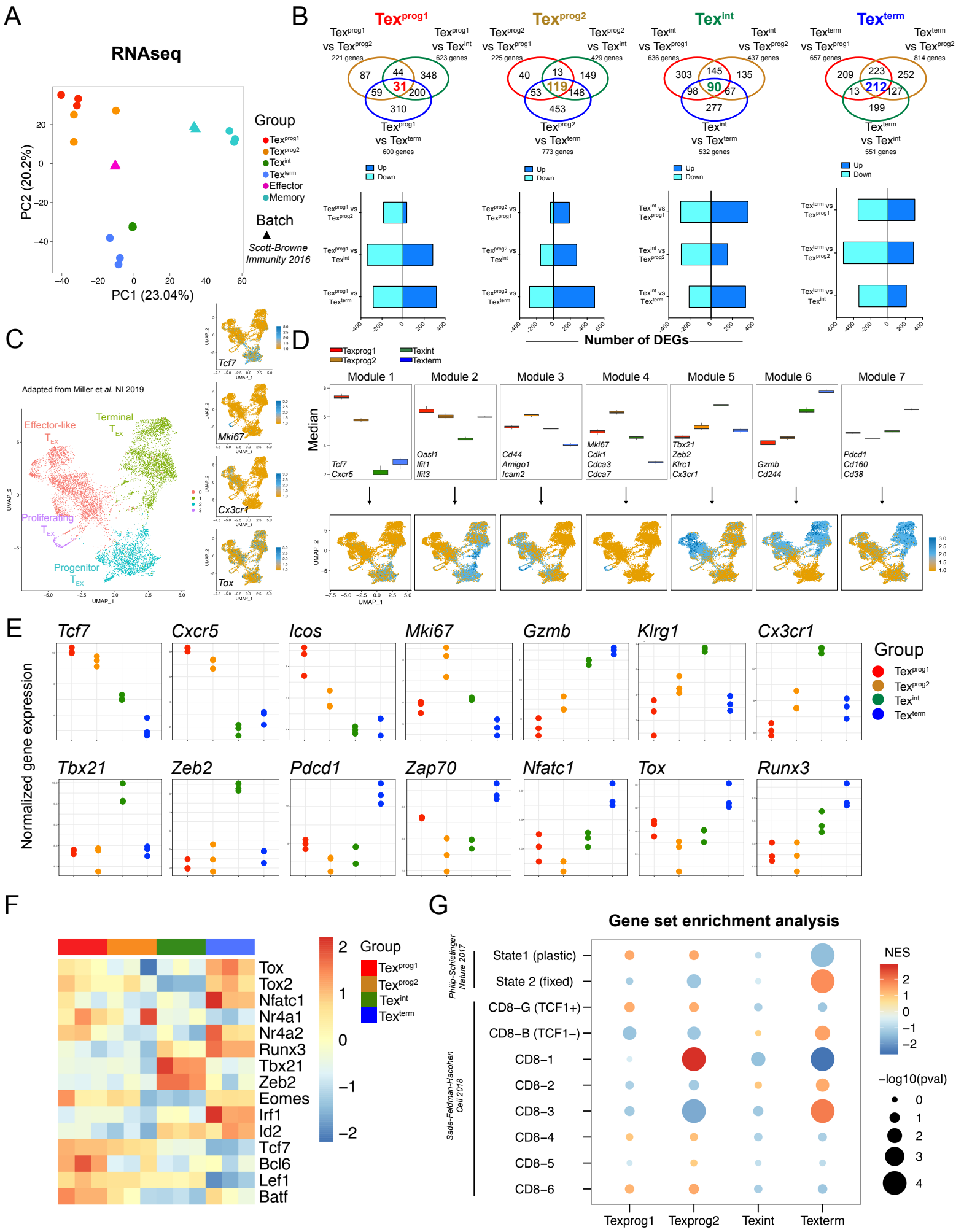

Figure. S5, related to main Figure 4: Transcriptional analysis of Tex subsets

(A) PCA of normalized RNAseq profiles. Each dot represents an independent experiment. (B) DEGs either up or down-regulated on indicated pairwise comparisons (lfc≥1, p.value=0.01). (C) Uniform Manifold Approximation and Projection (UMAP) representation of scRNAseq dataset of LCMV-derived Dbgp33^{+} Tex cells plotting previously described Tex clusters (left; Miller et *al*. NI 2019) or indicated genes (right). (D) Bi-clustering analysis of all DEGs from **Fig. 4b** identifying seven modules of genes (top row). Projection of each gene module into the scRNAseq UMAP from **Fig. S5c** (bottom row). (E) Normalized gene expression profiles of indicated genes in P14 cell populations. (F) Heatmap showing mRNA levels of selected TFs in the indicated Tex subsets. (G) GSEA comparing the transcriptional signature of each P14 population (compared to the three other subsets) to indicated cell types. NES stands for Normalized Enrichment Score.

(n=3 biological replicates)

Figure S6, related to main Figure 5.

(Legend next page)

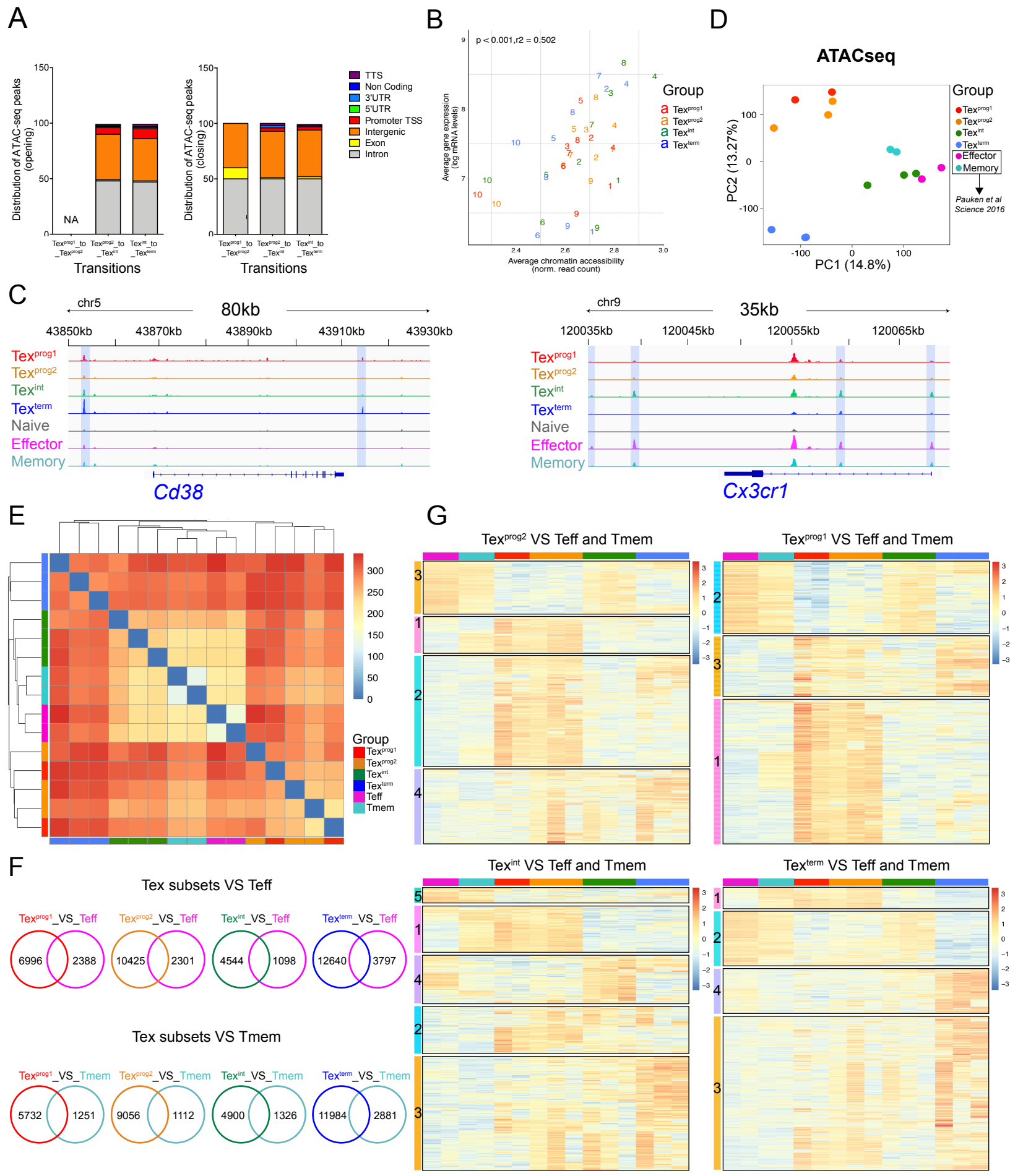

Figure. S6, related to main Figure 5: Epigenetic landscape of Tex subsets

(A) Bar graphs displaying the location of ATACseq peaks either opening (left histogram) or closing (right histogram) during indicated Tex subset transitions (lfc≥1, p.value<0.05). (B) Correlation between average gene expression (mRNA; from gene clusters defined in **Fig. 4d**) and average chromatin accessibility for each cluster in each sample. Numbers indicate gene clusters from **Fig. 4d**. (C) ATACseq tracks across the Cx3cr1 and Cd38 loci. (D) PCA of normalized ATACseq counts (all peaks). Each dot represents an independent experiment. (E) Sample distance analysis using the top 25% peaks by variance. Color legend indicates distances. (F) Differentially accessible peaks in indicated pairwise comparison (lfc≥2, p.value<0.01). (G) Heatmaps of peak intensity displaying the top 30% peaks differentially accessible in Tex^{prog1}, Tex^{prog2}, Tex^{int} or Tex^{term} compared with Teff and Tmem (lfc≥2, p.value<0.01).

(n=3 biological replicates)

Figure S7, related to main Figure 6 and 7.

(Legend next page)

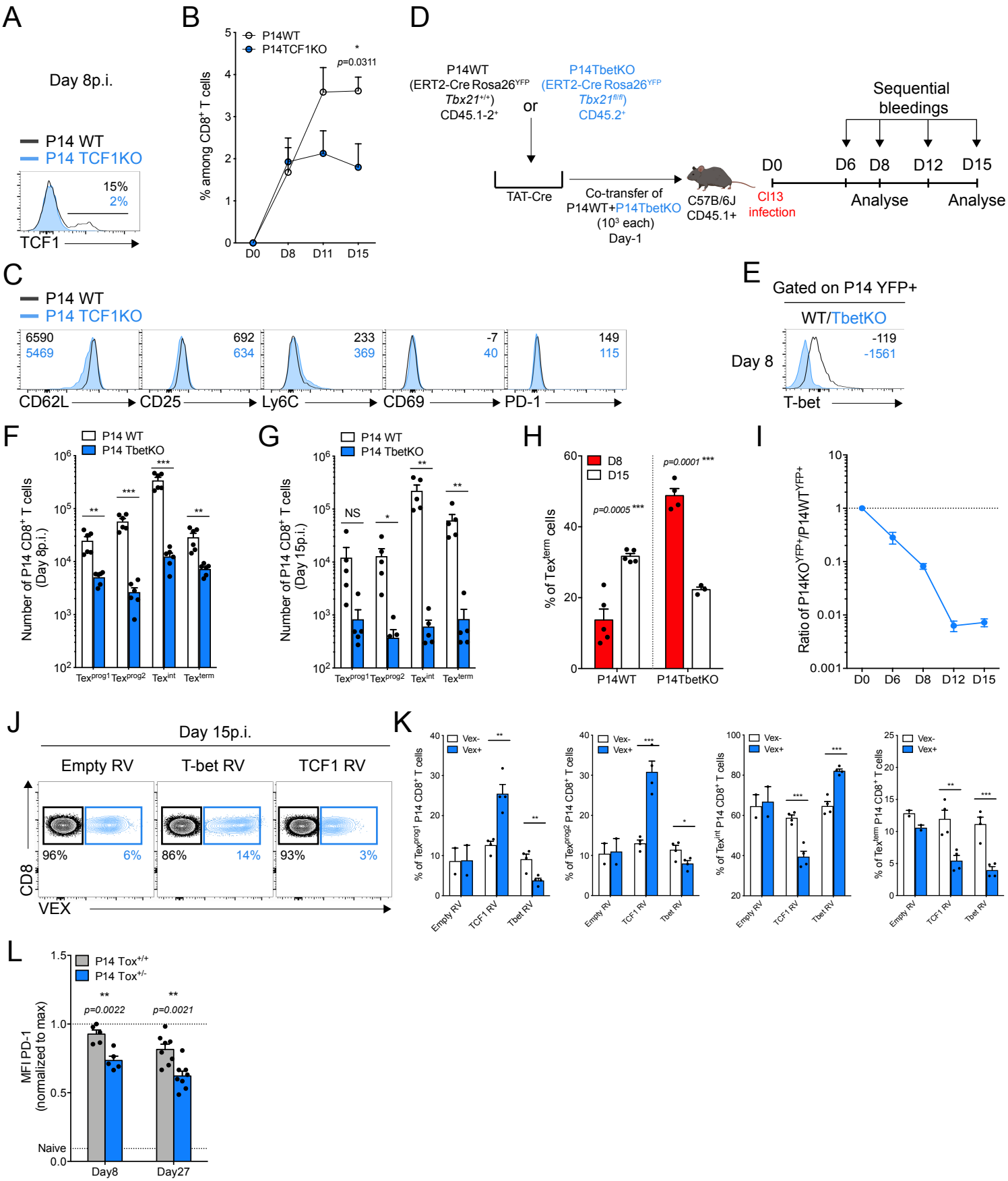

Figure. S7, related to main Figure 6 and 7: Interplay between TCF1, T-bet and Tox during Tex subset transitions

(A) Representative TCF1 expression in WT P14 (black) or TCF1KO P14 (blue) at d8p.i. Numbers indicate the frequency of positive cells. (B) Frequencies of WT P14 (open circle) and TCF1KO P14 (blue circle) in the blood of infected mice at the indicated time points. (C) Representative histograms showing the expression of indicated markers in naïve WT P14 (black) and TCF1KO P14 (blue) cells before adoptive transfer. Numbers indicate MFI. (D) Experimental design. *Tbx21*$^{fl/fl}$ ERT2-Cre$^{+/-}$ Rosa26-YFP$^{+/-}$ P14 (P14TbetKO) and their relative WT (*Tbx21*$^{+/+}$ ERT2-Cre$^{+/-}$ Rosa26-YFP$^{+/-}$) P14 controls were treated with TAT-cre *in vitro* to induce genetic recombination at the time of co-adoptive transfer (ratio 1:1) into LCMV clone 13 infected mice. Recombination was assessed *in vivo* by YFP expression and was routinely over 90%. (E) Representative T-bet expression in WT^{YFP+} P14 (black) and TbetKO^{YFP+} P14 (blue) cells at d8p.i. Numbers indicate MFI. (F-G) Absolute numbers of WT^{YFP+} P14 (open bars) and TbetKO^{YFP+} P14 (blue bars) cells in the spleen at d8 (F) or 15 (G) p.i. (H) Cumulative frequencies of Tex^{term} cells among WT^{YFP+} P14 and TbetKO^{YFP+} P14 cells at d8 (red bars) or 15 (open bars) p.i. (I) Graph displaying the ratio of TbetKO^{YFP+} P14 over WT^{YFP+} P14 cells in the blood of infected mice at indicated time points. (J) Representative flow cytometry plots displaying co-expression of CD8 and VEX on indicated P14 CD8^{+} T cell populations at d15p.i. Numbers indicate frequencies. (K) Frequencies of Tex^{prog1}, Tex^{prog2}, Tex^{int} and Tex^{term} cells at d15p.i. among the indicated P14 cell populations either transduced (blue bars) or not (open bars) with indicated RV constructs. (L) MFI of PD-1 on Tox$^{+/+}$ P14 (grey) or Tox$^{+/-}$ P14 (blue) cells at indicated time points.

Panels A-C (n=2 with 7 mice/group); E-I (Representative of 3-5 experiments with 11-17 mice/group); J-K (n=1 with 4 mice/group); L (Representative of 2 experiments with 15 mice/group)